

---

# Naive Few-Shot Learning: Sequence Consistency Evaluation

---

**Tomer Barak**

The Edmond and Lily Safra Center for Brain Sciences  
The Hebrew University, Jerusalem  
tomer.barak@mail.huji.ac.il

**Yonatan Loewenstein**

The Edmond and Lily Safra Center for Brain Sciences  
Department of Cognitive Sciences  
The Federmann Center for the Study of Rationality  
The Alexander Silberman Institute of Life Sciences  
The Hebrew University, Jerusalem  
yonatan.loewenstein@mail.huji.ac.il

## Abstract

Cognitive psychologists often use the term *fluid intelligence* to describe the ability of humans to solve novel tasks without any prior training. In contrast to humans, deep neural networks can perform cognitive tasks only after extensive (pre-)training with a large number of relevant examples. Motivated by fluid intelligence research in the cognitive sciences, we built a benchmark task which we call sequence consistency evaluation (SCE) that can be used to address this gap. Solving the SCE task requires the ability to extract simple rules from sequences, a basic computation that in humans, is required for solving various intelligence tests. We tested *untrained* (naive) deep learning models in the SCE task. Specifically, we tested two networks that can learn latent relations, Relation Networks (RN) and Contrastive Predictive Coding (CPC). We found that the latter, which imposes a causal structure on the latent relations performs better. We then show that naive few-shot learning of sequences can be successfully used for anomaly detection in two different tasks, visual and auditory, without any prior training.

## 1 Introduction

A hallmark of human intelligence is our constant attempt to find regularities or rules in the world around us. Intelligence tests are a standard tool for measuring humans' ability to find regularities without specific prior training, an ability that is often referred to as *fluid intelligence*. It has been demonstrated that deep learning models can successfully solve such tests (Santoro et al., 2017; Barrett et al., 2018; Zhuo & Kankanhalli, 2020; Kim et al., 2020). However, unlike humans, they require extensive prior training to achieve this goal. Are deep learning models capable of exhibiting "fluid intelligence"? To address this question, we noted that humans solve intelligence tests by dividing that task into distinct computational sub-problems and solving each of these separately (Sternberg, 1977, 1983; Lohman, 2000). A particularly important sub-problem that is shared among presumably different intelligence tests is the extraction of simple rules from sequences and their application for consistency evaluation (Siebers et al., 2015). For example, when solving a Raven's Progression Matrix (Raven et al., 1998), humans extract the rules governing the change in the matrix's rows and columns, and then use these rules to select the most consistent answer (Carpenter et al., 1990). Our

focus here is the extent to which naive models can solve this sub-problem, extracting simple rules from sequences without prior training. This is an unusual setting for deep learning models, in which pretraining is considered crucial even in the context of few-shot learning (Chollet, 2019; Vogelstein et al., 2022).

To that goal, we constructed a set of artificial problems in which the task is to evaluate the *consistency* of an input with a sequence of its preceding inputs based on a simple deterministic rule that is extracted from those preceding inputs. This sequence consistency evaluation (SCE) task can be used as a benchmark to study data-efficient machines. We compared the performance of the Contrastive Predictive Coding (CPC) and Relation Network (RN) models on this task without any pretraining. As consistency evaluation can be useful for detecting inconsistent anomalies, we applied the naive models to two anomaly detection tasks, of two different data modalities: videos from security cameras and auditory sounds from an office.

## 2 Relation to other works

**Intelligence tests solvers** Solving intelligence tests requires finding the features and the rules that govern them (Sternberg, 1977). Previous studies have shown that if the features are explicitly given, identifying the rule in intelligence tests is a relatively easy task, which can be solved without prior training (Carpenter et al., 1990; Rasmussen & Eliasmith, 2011). Deep learning models can solve intelligence tests without prior knowledge about the relevant features (Santoro et al., 2017; Barrett et al., 2018; Hill et al., 2019; Zhuo & Kankanhalli, 2020; Kim et al., 2020). However, unlike humans, these models rely on a large number of training examples to succeed, highlighting the data-efficiency gap between humans and machines.

**Few-shot learners** The primary approach today for achieving successful few-shot learning is to pretrain them over large relevant and diverse datasets and then fine-tune them for the new tasks (Brown et al., 2020; Reed et al., 2022). The problem with this approach is that the pretrained models have limited generalization ability to datasets that are different from the datasets they were trained on (Li et al., 2017; Nalisnick et al., 2019; Yin et al., 2020; Rajendran et al., 2020). Other modeling approaches achieved few-shot learning without pretraining. For example, one work utilized probabilistic program induction for naive handwritten character recognition (Lake et al., 2015). However, its success was based on pre-specified primitives. In another work, images were categorized using gradient descent over a pre-determined fixed set of simple image manipulations (Yu et al., 2022). Unlike these approaches, we use naive deep learning networks and study rule extraction in sequential data.

**Few-shot benchmarks** Meta-dataset is a dataset that groups several few-shot image classification datasets (Triantafillou et al., 2019). The meta-dataset tasks are too difficult to solve with an untrained deep learning model. Indeed, these datasets come with a large number of training examples that are used to pretrain models. The ARC dataset was designed to measure the fluid intelligence of naive models (Chollet, 2019), but it is also too challenging for today’s machines. Our benchmark tests evaluate models’ ability to tackle an easier sub-problem, whose solution can bring us closer to achieving naive few-shot deep learning.

## 3 Sequence consistency evaluation (SCE) tests

Each SCE test<sup>1</sup> is a sequences of  $K$  gray-scale images  $\mathbf{x}_j$  and  $n$  optional-choice images (Fig. 1). Each image includes 1-9 identical objects arranged on a  $3 \times 3$  grid. An image is characterized by a low-dimensional vector of features,  $\mathbf{f}_j$  where  $f_j^i$  denotes the value of feature  $i$  in image  $j$ . We use the following five features: the number of objects in an image (possible values: 1 to 9), their shade (6 linearly distributed grayscale values), the shapes (circle, triangle, square, star, hexagon), their size (6 linearly distributed values for the shapes’ enclosing circle circumference), and positions (a vector of grid positions that was used to place the shapes in order). An image  $\mathbf{x}_j$  is constructed according to its characterizing features by a non-linear and complex generative function  $\mathbf{x}_j = G(\mathbf{f}_j)$ .

<sup>1</sup>Code is available in the supplementary materials.

One of the features  $f^p$  predictably changes along the sequence according to a simple deterministic rule  $f_{j+1}^p = U(f_j^p)$  while the other features are either constant over the images or change randomly (values are i.i.d). We refer to the randomly-changing features as *distractors* and their number is considered a measure of the difficulty of the test. Given a sequence of  $K = 5$  images, an agent's task is to select the correct  $K + 1^{\text{th}}$  image from a set of  $n = 4$  optional choice images that are generated using the same generative function  $G$  from the feature space. In the correct choice,  $f^p$  follows the deterministic rule  $f_{K+1}^p = U(f_K^p)$ , whereas in the incorrect choices it does not follow that rule and is instead randomly chosen from the remaining possible values. The features that are constant or randomly changing in the sequence are also constant or change randomly in all optional choice images.

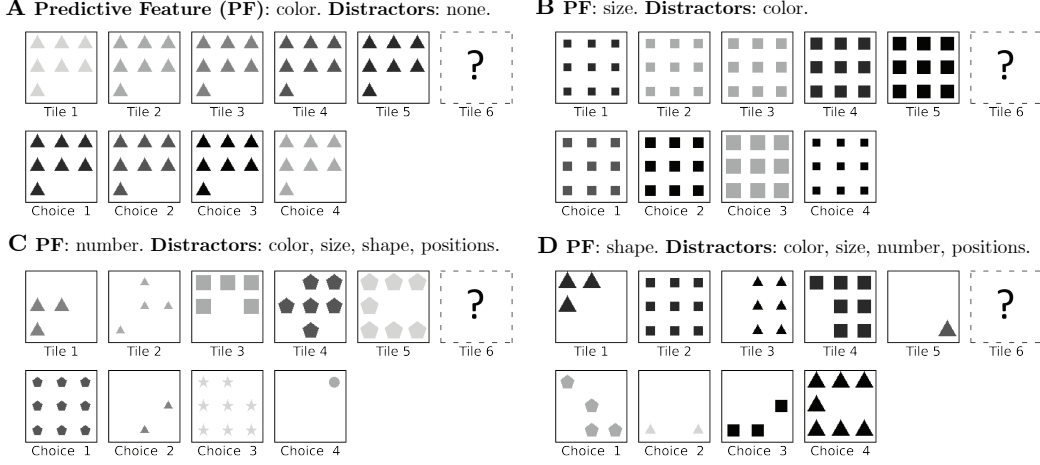


Figure 1: **SCE Tests.** The predictive features can be the (A) color, (B) size, (C) number which increases monotonically; or the (D) shape of the objects which alternates between a triangle and a square. Given a predictive feature, the rest of the features are either constant or random. We refer to the random features as *distractors* and their number determines the test difficulty. In all examples, the correct choice is 3.

## 4 Results

### 4.1 Two relation models

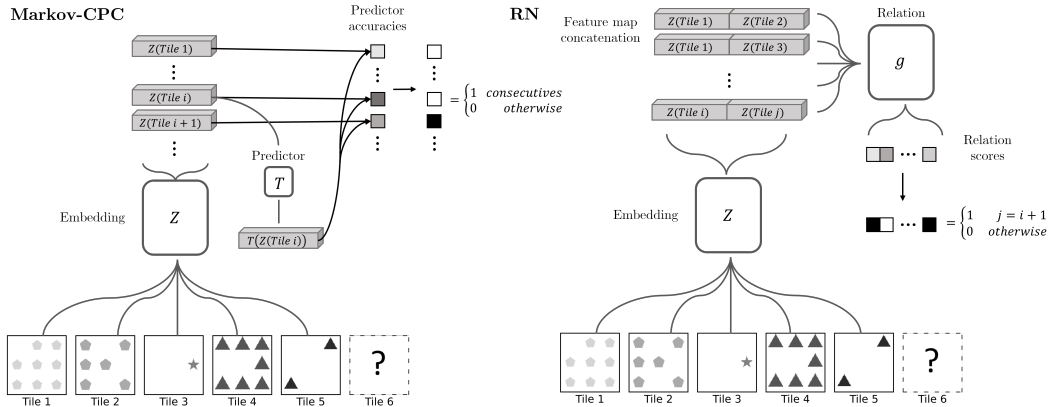


Figure 2: **Comparison between Markov-CPC (left) and RN (right).** The main difference between the models is that RN can learn a *general relation*  $g$  between two latent representations, while CPC imposes a *causal structure* between consecutive latent representations.

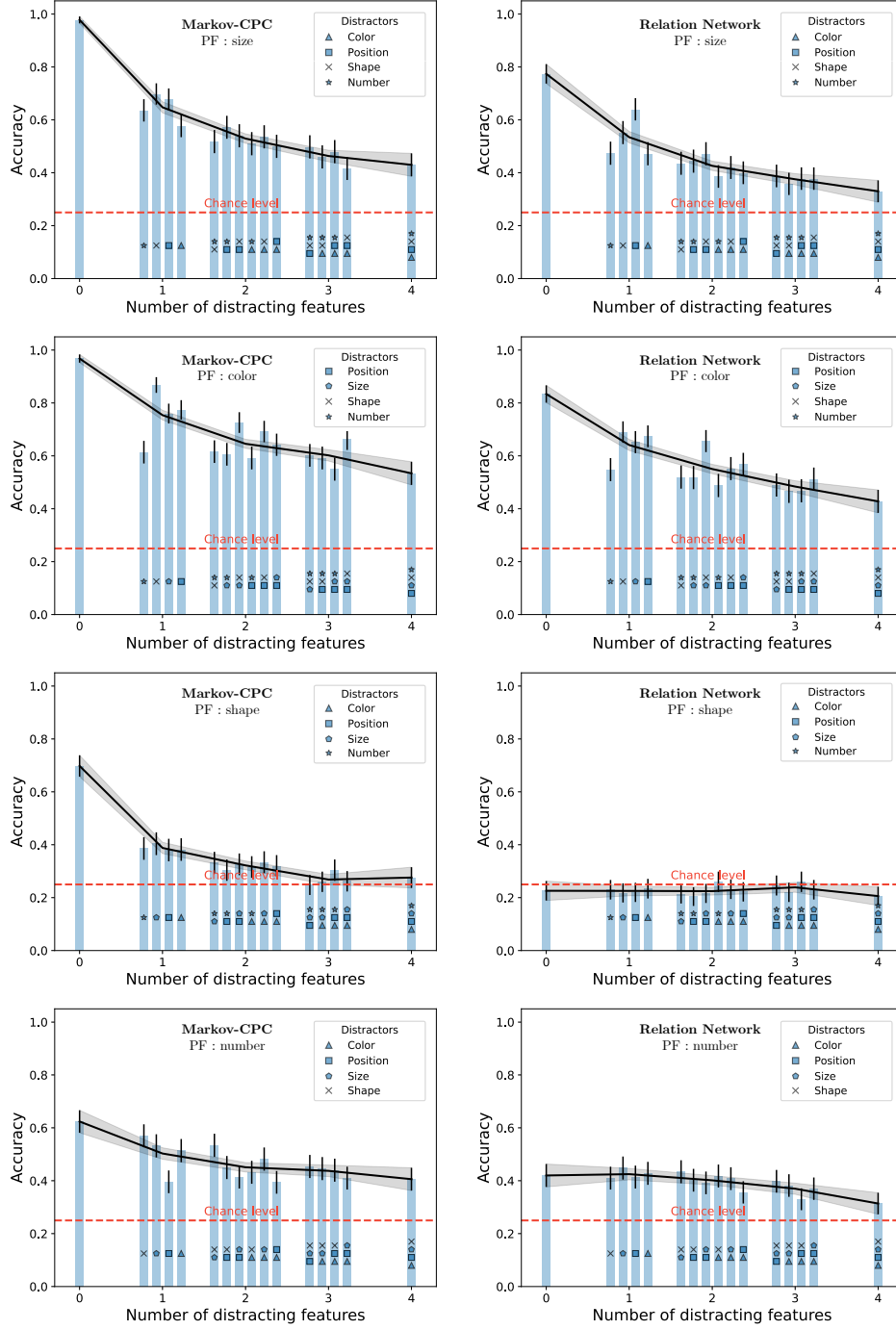


Figure 3: **Performance of the Markov-CPC (left column) and RN (right column) models on SCE tests with 4 different predictive features (rows).** For each predictive feature, we tested the networks over 16 test conditions where the rest of the features were either distractors (marked according to the legend) or constant (not marked). Each test condition included 500 randomly-generated intelligence tests. Error bars are 95% confidence intervals. The black line and its shade are the average accuracy per difficulty and the standard deviation. The dashed line denotes the chance level ( $\frac{1}{n}$ ).

The consistency in the SCE tests is determined by a latent relation between sequence images. We compared two main candidates of deep learning models that can extract latent relations from sequences: Contrastive Predictive Coding (CPC) (Oord et al., 2018) and Relation Network (RN) (Sung et al., 2018). Both models can be trained to classify whether two inputs are consecutive or not. RN learns to classify concatenations of two inputs’ latent variables with a *general* relation network  $g$  (Fig. 2 right). CPC, on the other hand, assumes a causal structure in the dynamics of the latent variable, where a predictor  $T$  predicts how a latent variable changes between two consecutive inputs (Fig. 2 left).

In this section, we use a variant of CPC called Markov-CPC. Unlike the original CPC that uses RNN to model possible non-Markovian relations between the latent variables, Markov-CPC prediction assumes that the dynamics of latent variables do not depend on their previous state. We also used a relatively shallow convolutional neural network for the encoder  $Z$  of both models.<sup>2</sup>

We applied the RN and Markov-CPC models to an SCE test in the following way: First, we randomly initialized the models’ networks. We then updated these networks’ weights with a *single* optimization step in the direction that minimizes the RN or Markov-CPC loss functions, given the five sequence images. After the single optimization step, we evaluated the consistency of each of the choice images with the sequence based on the resulting RN or Markov-CPC loss function, when these choices were applied as the sixth image. We selected the most consistent choice image, out of the  $n = 4$  choices, as the answer.

We found that the performance of the models reflects the difficulty of the tests, as defined by the number of distractors (Fig. 3). While both RN and Markov-CPC models exhibited better-than-chance performance in the easy tests and most of the difficult tests, Markov-CPC is superior to RN (average accuracies were  $0.52 \pm 0.02$  and  $0.42 \pm 0.02$  respectively). This result indicates that when trying to naively extract simple rules from sequences, it is beneficial to impose a causal latent structure.

Considering the CPC model, we found that the performance of a non-Markovian CPC, in which more complex relation between the latent variables is possible, is slightly worse than the Markov-CPC in this task. Additionally, we found that a) A residual  $T$  is better than a non-residual  $T$ ; b) The dimensionality of the latent variable is not a crucial parameter in these tests, and therefore, we used a 1-D latent variable; c) The contrastive loss in the loss function is important for the network performance; d) RMSprop optimizer seems to perform slightly better than SGD in this task; e) The relatively shallow network that we used for the encoder  $Z$  was found to be better than deeper and a more complicated networks in this task; f) Regarding the RN model, we also tested RN with its original deeper encoder, which has been proven useful in different few-shot image classification tasks (Sung et al., 2018). This RN model performed worse than with the simpler encoder, indicating that simpler networks may be better for this task. (see Appendix A3).

## 4.2 Prior training

The previous results established that Markov-CPC is an interesting model for naive few-shot learning. However, while performing substantially better than chance, it fails in selecting the correct choice image in many of the tests. To see whether this results from the limited expressivity of the model, we pretrained Markov-CPC with SCE tests as training episodes. Specifically, we performed one optimization step for each of these training episode tests and then tested the model on novel tests. We found that with 1000 training episodes, the performance of the Markov-CPC on tests in which size and color are the predictive features exceeds 90%, even in the hardest trials. These results indicate that at least for these predictive features, the performance of the Markov-CPC model is not limited by its expressivity. By contrast, when number or shape were the predictive features, performance level improved with training but only reached 60%–80%, leaving the question of expressivity of the model open.

---

<sup>2</sup>See appendix A1 for further model details.

Testing \ Training	Size (easy)	Size (hard)	Color (easy)	Color (hard)	Number (easy)	Number (hard)	Shape (easy)	Shape (hard)
Size (easy)	0.99 ±0.01	0.97 ±0.01	0.65 ±0.03	0.68 ±0.03	0.52 ±0.05	0.5 ±0.03	0.72 ±0.09	0.42 ±0.14
Size (hard)	0.9 ±0.0	0.88 ±0.01	0.24 ±0.0	0.25 ±0.01	0.24 ±0.01	0.24 ±0.01	0.32 ±0.04	0.31 ±0.04
Color (easy)	0.75 ±0.03	0.78 ±0.01	1.0 ±0.0	1.0 ±0.0	0.79 ±0.05	0.81 ±0.05	0.61 ±0.13	0.71 ±0.1
Color (hard)	0.26 ±0.01	0.27 ±0.01	0.93 ±0.01	0.95 ±0.01	0.27 ±0.01	0.26 ±0.01	0.53 ±0.03	0.34 ±0.05
Number (easy)	0.45 ±0.01	0.44 ±0.01	0.41 ±0.01	0.39 ±0.02	0.67 ±0.03	0.6 ±0.03	0.33 ±0.06	0.32 ±0.07
Number (hard)	0.26 ±0.0	0.26 ±0.01	0.28 ±0.01	0.25 ±0.01	0.7 ±0.02	0.67 ±0.03	0.33 ±0.03	0.26 ±0.04
Shape (easy)	0.18 ±0.02	0.25 ±0.03	0.29 ±0.02	0.33 ±0.03	0.2 ±0.02	0.26 ±0.03	0.37 ±0.06	0.31 ±0.05
Shape (hard)	0.24 ±0.01	0.25 ±0.01	0.26 ±0.01	0.26 ±0.0	0.24 ±0.01	0.25 ±0.01	0.27 ±0.01	0.24 ±0.02
Naive	0.97 ±0.0	0.42 ±0.01	0.96 ±0.0	0.55 ±0.01	0.60 ±0.01	0.40 ±0.01	0.71 ±0.0	0.26 ±0.01

Table 1: Accuracies presented are averaged over 10 experiments. In each experiment, a network was solving 500 intelligence tests in each of the 4 test conditions. The errors are the networks SEM.

Does pretraining in one type of test improve (or impair) the performance of another type of test? To address this question, we considered 8 different test types for training episodes (four different predictive features, either in the easiest setting of no distractors or in the hardest setting of four distractors) and tested the performance on those 8 different tests, yielding an  $8 \times 8$  performance matrix (Table. 1). The emerging picture is interesting. We find that training using easy episodes is typically more effective than training with hard ones within the same predictive feature. Interestingly, after training with the easy episodes, networks’ performance in the hard tests was comparable to their performance in the easy ones. Notably, pretraining on the predictive feature is not always effective. While effective when the predictive feature was the size, color, or number, it was detrimental relative to the naive case when the predictive feature was the shape (for which the predictive rule is qualitatively different from that of the other predictive features).

Typically (but not always), pretraining on one predictive feature was detrimental to the performance on tests characterized by a different predictive feature. This result highlights the potential advantage of a naive network over a trained one when the alignment between the training and testing domains is not perfect.

## 5 Anomaly detection

To test naive few-shot learning models in natural settings, in which alternative choice images may be lacking, and compare the performance of Markov-CPC and RN, we tested the abilities of these models to detect unlabeled anomalies in two datasets.

The first dataset, UMN (Mehran et al., 2009), consists of 11 security camera videos that A) start with humans walking normally; B) towards the end of the videos they start running; C) a label of "Abnormal Crowd Activity" appears shortly after<sup>3</sup> (Fig. 4 A-C).

<sup>3</sup>In the tests we removed the top 30 pixels of all images to exclude this label.

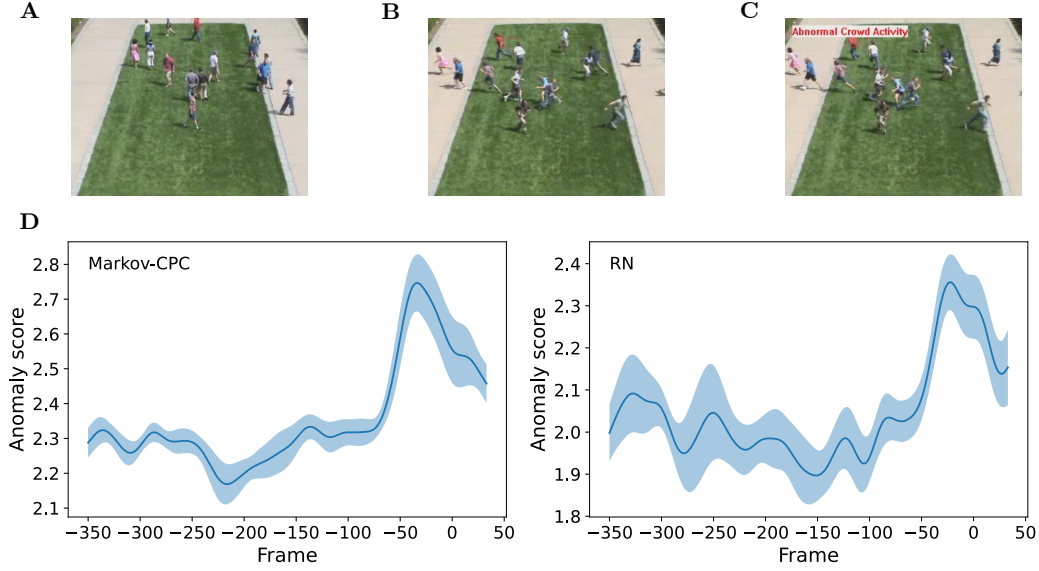


Figure 4: **UMN Anomaly scores.** (A-C) Example frames from the first UMN video: (A) normal walking human behavior; (B) humans start to run; (C) “Abnormal Crowd Activity” label appears. (D) Anomaly scores of the frames. The frames are numbered with respect to the first appearance of the “Abnormal Crowd Activity” label. We ran a model 5 times for each frame. We averaged the anomaly scores over the 5 runs per frame and smoothed the scores with a Gaussian kernel with a standard deviation of 10 frames. Finally, we averaged the resulting scores over the 11 videos.

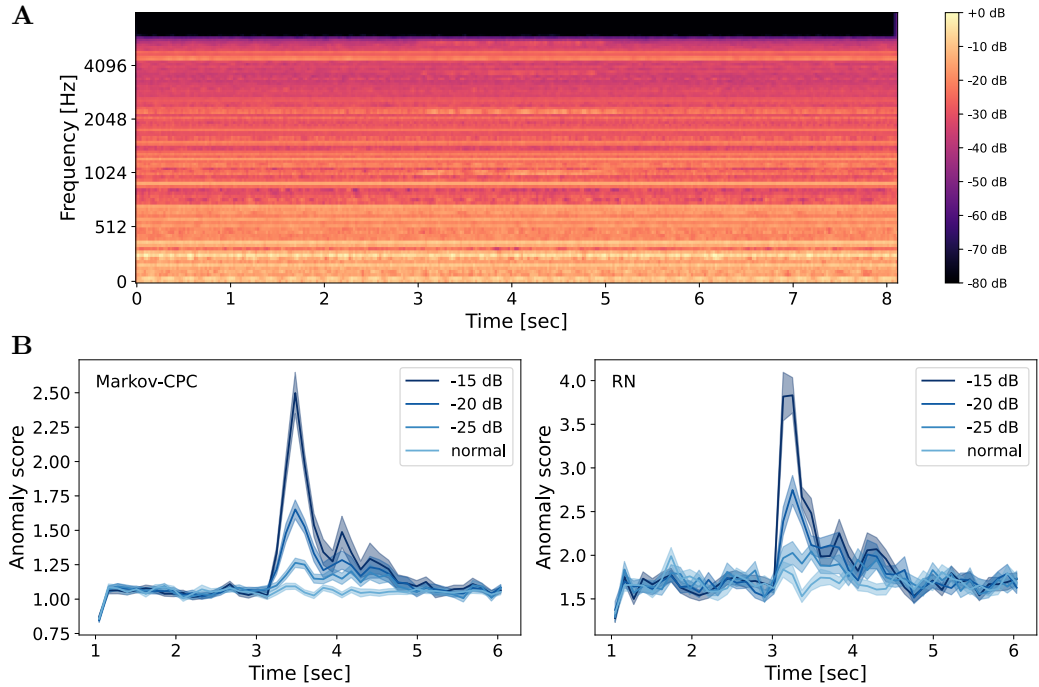


Figure 5: **ADS anomaly scores.** (A) Example spectrogram of a phone that rings over natural background noise. The anomaly-to-noise (ANR) ratio in this example is -20 dB. (B) Anomaly scores, obtained by Markov-CPC and RN. We averaged the anomaly scores over 5 iterations per frame of each sound snippet and the 140 sound snippets in each ANR.

We assigned each video frame with an anomaly score that is based on its consistency with its five preceding frames (see details in appendix A2). We found that both the Markov-CPC and the RN models assigned larger anomaly scores to the frames in which the humans started to run (Fig. 4). Detecting the time in which running begins is not a difficult task for trained networks and previous anomaly detection models achieved nearly perfect scores in this dataset (Pang et al., 2020). However, these previous models all relied on prior training. By contrast, our objective was to identify these anomalies without any prior training.

The second dataset, Anomaly Detection of Sound (ADS) (Koizumi et al., 2019) consists of 140 short sound snippets. Each snippet is made of natural background noise, such as the noise of an air conditioner recorded in a natural environment, interrupted by various types of anomalous sounds, such as keys falling or a drawer closing. The detection difficulty was controlled by the anomaly-to-noise power ratios (ANRs) which were set to -15 dB, -20 dB, or -25 dB. This dataset is more challenging, and even trained networks fail in detecting the anomalous sounds in some examples.

To test our models on this dataset, we converted the sound snippets into a video in which each frame was a Mel-spectrogram window of  $\sim 0.5$  seconds of the snippet, hopped in  $\sim 0.1$  second steps. Then, similar to the analysis of the UMN dataset, we computed an anomaly score for each image based on the previous five frames using either the Markov-CPC or the RN models. As shown in Fig. 5, both models assigned relatively higher anomaly scores to anomalous events.

To compare our results with other models, we used the standard AUC measure (area under the ROC curve) (Pedregosa et al., 2011) based on the maximal anomaly score of each snippet. For Markov-CPC The AUC scores were around 0.96, 0.84, and 0.67 for the -15, -20, and -25 dB ANRs respectively, values that are comparable to previous, even though previous models require prior training while the Markov-CPC model is naive (Fig. 6). The RN model exhibited substantially poorer performance in this task than the Markov-CPC model. The finding that the Markov-CPC model performs better than the RN model is consistent with its relative success in the SCE tests.

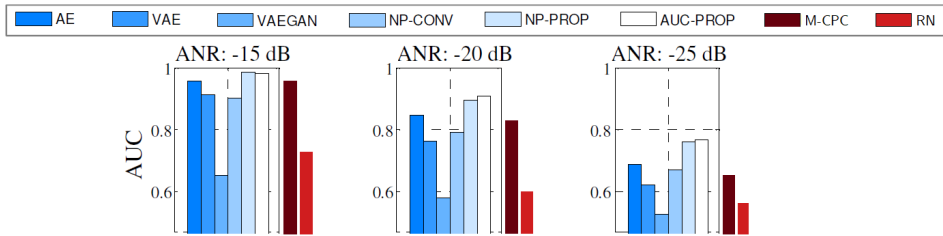


Figure 6: **Model comparison.** AUC scores for anomaly detection of different models. Bars in the boxes depict the AUC scores of six models that require prior training (adapted from (Koizumi et al., 2019)). Darker and lighter red depict the AUC scores of the Markov-CPC and RN models, respectively. The performance of the Markov-CPC model in this task is comparable to that of previous models, even though it does not require any training.

## 6 Discussion

Motivated by the data-efficiency gap between humans and deep learning models, we focused on rule extraction, an important component of humans’ fluid intelligence. We created a benchmark of SCE tests, which can be used to test agents’ ability to extract rules. We then tested the ability of models to solve these tests. In contrast to the standard few-shot learning approach, which utilizes extensive prior training, we tested the ability of naive models, without any prior training, to solve the SCE tests. We found that surprisingly, deep learning models that can find latent relations can successfully solve these tasks. Moreover, a Markov-CPC model, which imposes a causal latent structure on the rules, performs better than a more general RN model that does not impose such a structure. To study the applicability of these results, we applied the two models to two anomaly detection tasks. As with the SCE tests, the Markov-CPC model performed better than the RN model. Remarkably, the



Markov-CPC model’s performance was comparable to that of pretrained models, demonstrating the potential of naive models in addressing real-world problems.

**Limitations.** a) To test whether the performance on the SCE tests was limited by the expressivity of Markov-CPC, we pretrained Markov-CPC on these tests. We found that it achieved perfect performance in the color and size rules, indicating that it is expressive enough to represent these rules. However, Markov-CPC achieved only 60%-80% performance in the number and shape rules, keeping open the question as to whether this model is expressive enough to fully learn these rules. b) The SCE tests include only Markovian rules. This suggests that high-performing models in the SCE tests might not be able to find non-Markovian regularities such as logical gates. However, this limitation can be overcome by a Markovian representation of non-Markovian dynamics, e.g., by state representations that encompass more than one time steps.

**Flexible anomaly detection.** The fact that the model does not require any prior training allowed us to apply it with only minor adaptations directly to a problem that is very different from the SCE task, anomaly detection. Moreover, it also enabled us to use the exactly same code to detect anomalies in two very different datasets, in a visual sequence from a security camera and in an auditory sequence hidden in background noise. These results demonstrate the utility of this framework for identifying unforeseeable abnormalities. Moreover, because the effective networks are shallow (see table t7 in the appendix), and because it takes just one gradient step to detect an anomaly, these models are fast. Indeed, the Markov-CPC can solve 13 SCE tasks per second on a simple computer. Together, these results suggest that naive few-shot learning can be used as a flexible anomaly detection device (like Spider-Man’s spider-sense) (Table 2).

**Further applications of naive few-shot learning.** A promising direction will be to combine naive models as part of a composite system. For example, it might be possible to train the data-efficient Markov-CPC using incremental few-shot learning methods (Tao et al., 2020; Jin et al., 2021; Zhang et al., 2021) and achieve improvement in a specific task while retaining the model’s general fluid ability. Another possibility, inspired by the way that humans solve intelligence tests such as Raven Progression Matrices (Sternberg, 1977; Carpenter et al., 1990; Raven et al., 1998), is to combine a naive model with planning, working memory, and generative mechanisms.

**SCE tests application.** As naive models need to be flexible to apply to various datasets out-of-the-box, a standard evaluation test of their ability will be useful. In our experiments, the performance of the models in the SCE tests was consistent with their anomaly detection performance. This suggests the SCE tests as a candidate benchmark for evaluating naive models’ general fluid rule-extraction ability.

**Summary.** A limiting factor to the use of deep networks is that they typically require large datasets and computationally-expensive training to effectively solve computational problems. Even when these conditions are met, the resulting networks become task-specific. By contrast, naive, or nearly-naive models do not suffer from these shortcomings (Table 2). In a field that is dominated by extensive training with an extensive number of examples, our work demonstrates the potential power of naive networks. We believe that pursuing this line of research, making data-efficient artificial neural networks, will bring machine intelligence closer to that of humans.

	Pretrained models	Naive models
Accuracy	Accurate	Inaccurate
Generality	Specific	General
Data	Expensive	Cheap
Training time	Long	Short

Table 2: The trade-off between extensively pretrained and naive models.

## Acknowledgments and Disclosure of Funding

This work was supported by the Israel Science Foundation (Grant No. 757/16) and the Gatsby Charitable Foundation. This work is dedicated to the memory of Mrs. Lily Safra, a great supporter of brain research.

## References

- Anand, A., Racah, E., Ozair, S., Bengio, Y., Côté, M.-A., and Hjelm, R. D. Unsupervised State Representation Learning in Atari. (NeurIPS), 2019. URL <http://arxiv.org/abs/1906.08226>.
- Barrett, D. G. T., Hill, F., Santoro, A., Morcos, A. S., and Lillicrap, T. Measuring abstract reasoning in neural networks. 2018. ISSN 17740746. doi: 10.1051/agro/2009059. URL <http://arxiv.org/abs/1807.04225>. ISBN: 1807.04225v1.
- Brown, T. B., Mann, B., Ryder, N., Subbiah, M., Kaplan, J., Dhariwal, P., Neelakantan, A., Shyam, P., Sastry, G., Askell, A., Agarwal, S., Herbert-Voss, A., Krueger, G., Henighan, T., Child, R., Ramesh, A., Ziegler, D. M., Wu, J., Winter, C., Hesse, C., Chen, M., Sigler, E., Litwin, M., Gray, S., Chess, B., Clark, J., Berner, C., McCandlish, S., Radford, A., Sutskever, I., and Amodei, D. Language Models are Few-Shot Learners. Technical Report arXiv:2005.14165, arXiv, July 2020. URL <http://arxiv.org/abs/2005.14165>. arXiv:2005.14165 [cs] type: article.
- Carpenter, P. A., Just, M. A., and Shell, P. What One Intelligence Test Measures: A Theoretical Account of the Processing in the Raven Progressive Matrices Test. (3):28, 1990.
- Chollet, F. On the Measure of Intelligence. *arXiv:1911.01547 [cs]*, November 2019. URL <http://arxiv.org/abs/1911.01547>. arXiv: 1911.01547.
- He, K., Zhang, X., Ren, S., and Sun, J. Deep residual learning for image recognition. In *Proceedings of the IEEE conference on computer vision and pattern recognition*, pp. 770–778, 2016.
- Henaff, O. Data-Efficient Image Recognition with Contrastive Predictive Coding. In *Proceedings of the 37th International Conference on Machine Learning*, pp. 4182–4192. PMLR, November 2020. URL <https://proceedings.mlr.press/v119/henaff20a.html>. ISSN: 2640-3498.
- Hill, F., Santoro, A., Barrett, D. G. T., Morcos, A. S., and Lillicrap, T. Learning to Make Analogies by Contrasting Abstract Relational Structure. 2019. URL <http://arxiv.org/abs/1902.00120>.
- Hochreiter, S. and Schmidhuber, J. Long Short-Term Memory. *Neural Computation*, 9(8):1735–1780, November 1997. ISSN 0899-7667. doi: 10.1162/neco.1997.9.8.1735. Conference Name: Neural Computation.
- Howard, A. G., Zhu, M., Chen, B., Kalenichenko, D., Wang, W., Weyand, T., Andreetto, M., and Adam, H. Mobilenets: Efficient convolutional neural networks for mobile vision applications. *arXiv preprint arXiv:1704.04861*, 2017.
- Huang, G., Liu, Z., Van Der Maaten, L., and Weinberger, K. Q. Densely connected convolutional networks. In *Proceedings of the IEEE conference on computer vision and pattern recognition*, pp. 4700–4708, 2017.
- Jin, X., Lin, B. Y., Rostami, M., and Ren, X. Learn continually, generalize rapidly: Lifelong knowledge accumulation for few-shot learning. *arXiv preprint arXiv:2104.08808*, 2021.
- Kim, Y., Shin, J., Yang, E., and Hwang, S. J. Few-shot Visual Reasoning with Meta-analogical Contrastive Learning. *arXiv:2007.12020 [cs, stat]*, July 2020. URL <http://arxiv.org/abs/2007.12020>. arXiv: 2007.12020.
- Koizumi, Y., Saito, S., Uematsu, H., Kawachi, Y., and Harada, N. Unsupervised Detection of Anomalous Sound Based on Deep Learning and the Neyman–Pearson Lemma. *IEEE/ACM Transactions on Audio, Speech, and Language Processing*, 27(1):212–224, January 2019. ISSN 2329-9304. doi: 10.1109/TASLP.2018.2877258. Conference Name: IEEE/ACM Transactions on Audio, Speech, and Language Processing.
- Krizhevsky, A., Sutskever, I., and Hinton, G. E. Imagenet classification with deep convolutional neural networks. In Pereira, F., Burges, C., Bottou, L., and Weinberger, K. (eds.), *Advances in Neural Information Processing Systems*, volume 25. Curran Associates, Inc., 2012. URL <https://proceedings.neurips.cc/paper/2012/file/c399862d3b9d6b76c8436e924a68c45b-Paper.pdf>.

- Lake, B. M., Salakhutdinov, R., and Tenenbaum, J. B. Human-level concept learning through probabilistic program induction. *Science*, 350(6266):1332–1338, December 2015. doi: 10.1126/science.aab3050. URL <https://www.science.org/doi/10.1126/science.aab3050>. Publisher: American Association for the Advancement of Science.
- Li, D., Yang, Y., Song, Y.-Z., and Hospedales, T. M. Learning to Generalize: Meta-Learning for Domain Generalization. *arXiv:1710.03463 [cs]*, October 2017. URL <http://arxiv.org/abs/1710.03463>. arXiv: 1710.03463.
- Lohman, D. F. Complex Information Processing and Intelligence. In Sternberg, R. J. (ed.), *Handbook of Intelligence*, pp. 285–340. Cambridge University Press, Cambridge, 2000. ISBN 978-0-521-59648-0. doi: 10.1017/CBO9780511807947.015.
- Mehran, R., Oyama, A., and Shah, M. Abnormal crowd behavior detection using social force model. In *2009 IEEE Conference on Computer Vision and Pattern Recognition*, pp. 935–942, June 2009. doi: 10.1109/CVPR.2009.5206641. URL [http://mha.cs.umn.edu/proj\\_events.shtml#crowd](http://mha.cs.umn.edu/proj_events.shtml#crowd). ISSN: 1063-6919.
- Nalisnick, E., Matsukawa, A., Teh, Y. W., Gorur, D., and Lakshminarayanan, B. Do Deep Generative Models Know What They Don’t Know? Technical Report arXiv:1810.09136, arXiv, February 2019. URL <http://arxiv.org/abs/1810.09136>. arXiv:1810.09136 [cs, stat] type: article.
- Oord, A. v. d., Li, Y., and Vinyals, O. Representation Learning with Contrastive Predictive Coding. 2018. URL <http://arxiv.org/abs/1807.03748>.
- Pang, G., Yan, C., Shen, C., Hengel, A. v. d., and Bai, X. Self-Trained Deep Ordinal Regression for End-to-End Video Anomaly Detection. pp. 12173–12182, 2020. URL [https://openaccess.thecvf.com/content\\_CVPR\\_2020/html/Pang\\_Self-Trained\\_Deep\\_Ordinal\\_Regression\\_for\\_End-to-End\\_Video\\_Anomaly\\_Detection\\_CVPR\\_2020\\_paper.html](https://openaccess.thecvf.com/content_CVPR_2020/html/Pang_Self-Trained_Deep_Ordinal_Regression_for_End-to-End_Video_Anomaly_Detection_CVPR_2020_paper.html).
- Pedregosa, F., Varoquaux, G., Gramfort, A., Michel, V., Thirion, B., Grisel, O., Blondel, M., Prettenhofer, P., Weiss, R., Dubourg, V., et al. Scikit-learn: Machine learning in python. *Journal of machine learning research*, 12(Oct):2825–2830, 2011.
- Rajendran, J., Irpan, A., and Jang, E. Meta-Learning Requires Meta-Augmentation. In Larochelle, H., Ranzato, M., Hadsell, R., Balcan, M. F., and Lin, H. (eds.), *Advances in Neural Information Processing Systems*, volume 33, pp. 5705–5715. Curran Associates, Inc., 2020. URL <https://proceedings.neurips.cc/paper/2020/file/3e5190eeb51ebe6c5bbc54ee8950c548-Paper.pdf>.
- Rasmussen, D. and EliaSmith, C. A neural model of rule generation in inductive reasoning. *Topics in Cognitive Science*, 3(1):140–153, 2011. ISSN 17568757. doi: 10.1111/j.1756-8765.2010.01127.x.
- Raven, J., Raven, J. C., and Court, J. H. *Manual for Raven’s progressive matrices and vocabulary scales*. Pearson, San Antonio, TX, 1998. ISBN 978-0-15-868643-1 978-0-15-468622-0 978-0-15-468623-7 978-1-85639-022-4. OCLC: 697438611.
- Reed, S., Zolna, K., Parisotto, E., Colmenarejo, S. G., Novikov, A., Barth-Maron, G., Gimenez, M., Sulsky, Y., Kay, J., Springenberg, J. T., Eccles, T., Bruce, J., Razavi, A., Edwards, A., Heess, N., Chen, Y., Hadsell, R., Vinyals, O., Bordbar, M., and de Freitas, N. A Generalist Agent. Technical Report arXiv:2205.06175, arXiv, May 2022. URL <http://arxiv.org/abs/2205.06175>. arXiv:2205.06175 [cs] type: article.
- Santoro, A., Raposo, D., Barrett, D. G. T., Malinowski, M., Pascanu, R., Battaglia, P., and Lillicrap, T. A simple neural network module for relational reasoning. *Advances in Neural Information Processing Systems*, 2017-Decem:4968–4977, 2017. ISSN 10495258.
- Siebers, M., Dowe, D. L., Schmid, U., Hernández-Orallo, J., and Martínez-Plumed, F. Computer models solving intelligence test problems: Progress and implications. *Artificial Intelligence*, 230: 74–107, 2015. ISSN 00043702. doi: 10.1016/j.artint.2015.09.011. URL <http://dx.doi.org/10.1016/j.artint.2015.09.011>. ISBN: 9780999241103 Publisher: Elsevier B.V.

- Simonyan, K. and Zisserman, A. Very deep convolutional networks for large-scale image recognition. *arXiv preprint arXiv:1409.1556*, 2014.
- Sternberg, R. J. Component processes in analogical reasoning. *Psychological Review*, 84(4):353–378, 1977. ISSN 0033295X. doi: 10.1037/0033-295X.84.4.353.
- Sternberg, R. J. Components of human intelligence. *Cognition*, 15(1-3):1–48, 1983. ISSN 00100277. doi: 10.1016/0010-0277(83)90032-X.
- Sung, F., Yang, Y., Zhang, L., Xiang, T., Torr, P. H. S., and Hospedales, T. M. Learning to Compare: Relation Network for Few-Shot Learning. pp. 1199–1208, 2018. URL [https://openaccess.thecvf.com/content\\_cvpr\\_2018/html/Sung\\_Learning\\_to\\_Compare\\_CVPR\\_2018\\_paper.html](https://openaccess.thecvf.com/content_cvpr_2018/html/Sung_Learning_to_Compare_CVPR_2018_paper.html).
- Tao, X., Hong, X., Chang, X., Dong, S., Wei, X., and Gong, Y. Few-shot class-incremental learning. In *Proceedings of the IEEE/CVF Conference on Computer Vision and Pattern Recognition*, pp. 12183–12192, 2020.
- Triantafillou, E., Zhu, T., Dumoulin, V., Lamblin, P., Evci, U., Xu, K., Goroshin, R., Gelada, C., Swersky, K., Manzagol, P.-A., and Larochelle, H. Meta-Dataset: A Dataset of Datasets for Learning to Learn from Few Examples. September 2019. URL <https://openreview.net/forum?id=rkgAGAVKPr>.
- Vogelstein, J. T., Verstynen, T., Kording, K. P., Isik, L., Krakauer, J. W., Etienne-Cummings, R., Ogburn, E. L., Priebe, C. E., Burns, R., Kuten, K., Knierim, J. J., Potash, J. B., Hartung, T., Smirnova, L., Worley, P., Savonenko, A., Phillips, I., Miller, M. I., Vidal, R., Sulam, J., Charles, A., Cowan, N. J., Bichuch, M., Venkataraman, A., Li, C., Thakor, N., Kebschull, J. M., Albert, M., Xu, J., Shuler, M. H., Caffo, B., Ratnanather, T., Geisa, A., Roh, S.-E., Yezerets, E., Madhyastha, M., How, J. J., Tomita, T. M., Dey, J., Ningyuan, Huang, Shin, J. M., Kinfu, K. A., Chaudhari, P., Baker, B., Schapiro, A., Jayaraman, D., Eaton, E., Platt, M., Ungar, L., Wehbe, L., Kepecs, A., Christensen, A., Osuagwu, O., Brunton, B., Mensh, B., Muotri, A. R., Silva, G., Puppo, F., Engert, F., Hillman, E., Brown, J., White, C., and Yang, W. Prospective Learning: Back to the Future. *arXiv:2201.07372 [cs]*, January 2022. URL <http://arxiv.org/abs/2201.07372>. arXiv: 2201.07372.
- Yan, W., Vangipuram, A., Abbeel, P., and Pinto, L. Learning Predictive Representations for Deformable Objects Using Contrastive Estimation. 2020. URL <http://arxiv.org/abs/2003.05436>.
- Yin, M., Tucker, G., Zhou, M., Levine, S., and Finn, C. Meta-Learning without Memorization. *arXiv:1912.03820 [cs, stat]*, April 2020. URL <http://arxiv.org/abs/1912.03820>. arXiv: 1912.03820.
- Yu, H., Mineyev, I., Varshney, L. R., and Evans, J. A. Learning from One and Only One Shot. *arXiv:2201.08815 [cs]*, January 2022. URL <http://arxiv.org/abs/2201.08815>. arXiv: 2201.08815.
- Zhang, C., Song, N., Lin, G., Zheng, Y., Pan, P., and Xu, Y. Few-shot incremental learning with continually evolved classifiers. In *IEEE/CVF Conference on Computer Vision and Pattern Recognition (CVPR)*, June 2021.
- Zhuo, T. and Kankanhalli, M. Solving Raven’s Progressive Matrices with Neural Networks. *arXiv:2002.01646 [cs]*, February 2020. URL <http://arxiv.org/abs/2002.01646>. arXiv: 2002.01646.

## Appendix

### A1 Models details

#### A1.1 Markov-CPC

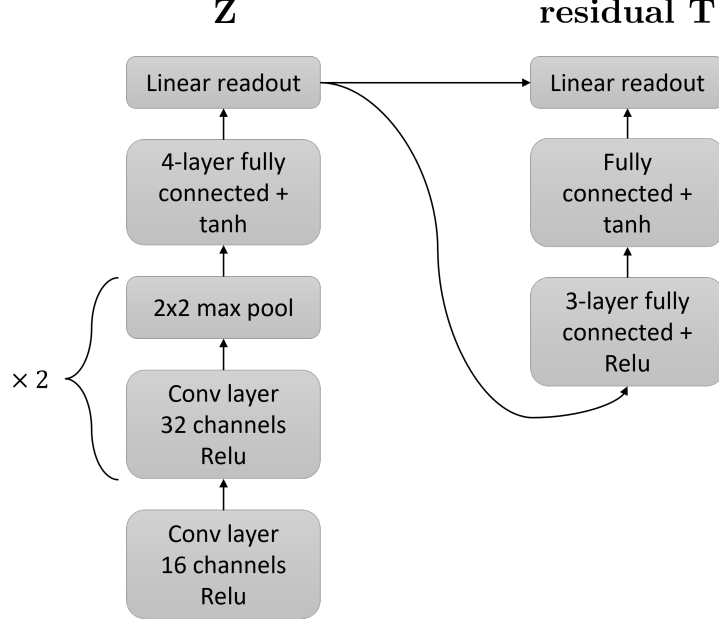


Figure f1: **M-CPC architecture.**

Markov-CPC is a variant of the Contrastive Predictive Coding (CPC) algorithm (Oord et al., 2018) which was shown useful for finding predictive latent variables (Anand et al., 2019; Henaff, 2020; Yan et al., 2020). This self-supervised algorithm optimizes an infoNCE loss in which consecutive inputs in a sequence are regarded as positive examples and non-consecutive inputs as negative examples.

Our main challenge in solving the intelligence tests is to find a latent variable that changes in a simple deterministic way along the test’s five image sequence. Consider an encoder function  $Z$ , a predictor function  $T$ , two images  $\mathbf{x}_a$  and  $\mathbf{x}_b$  and the prediction error

$$\epsilon_{a,b}(Z, T) = \left( T(Z(\mathbf{x}_a)) - Z(\mathbf{x}_b) \right)^2 \quad (1)$$

By construction, for the true encoder and predictor functions  $Z^* = G^{-1}$  and  $T^* = U$ ,  $\epsilon_{a,b}(Z^*, T^*) = 0$  if  $a$  and  $b$  are two consecutive images ( $b = a + 1$ ), and  $\epsilon_{a,b}(Z^*, T^*) \neq 0$  otherwise.

The challenge is that  $Z^*$  and  $T^*$  are unknown. However, given a sequence of  $K$  ordered images, we can approximate  $Z^*$  and  $T^*$  by finding  $Z$  and  $T$  that minimize the prediction error for consecutive images and maximize it for the non-consecutive ones. Formally, we define a contrastive infoNCE loss based on those prediction errors

$$\mathcal{L} = -\frac{1}{K-1} \sum_{j=1}^{K-1} \log \frac{e^{-\epsilon_{j,j+1}}}{\sum_{j'} e^{-\epsilon_{j,j'}}} \quad (2)$$

and find  $Z$  and  $T$  that minimize it.

Markov-CPC’s encoder  $Z$  and predictor  $T$  are implemented by deep neural networks (Fig. f1). For the predictor  $T$ , we used a residual network, such that

$$T(Z(\mathbf{x})) = Z(\mathbf{x}) + \Delta T(Z(\mathbf{x}))$$

where  $\Delta T$  is a fully connected neural network.

For the optimization steps, we used the RMSprop optimizer with a learning rate  $\eta = 4 \cdot 10^{-4}$ . The rest of the optimizer hyperparameters were set to PyTorch default.

### A1.2 Relation Network

We used the same Relation Network loss function as in the original paper (Sung et al., 2018). For the networks, we either used the networks from (Sung et al., 2018) or used the same  $Z$  and  $g$  as Markov-CPC. In both cases, we used the RMSprop optimizer. For the original RN networks from (Sung et al., 2018) we used a learning of  $\eta = 4 \cdot 10^{-6}$ . When we used the  $Z$  of Markov-CPC, we used the learning rate  $\eta = 4 \cdot 10^{-4}$ . The rest of the optimizer parameters were set to PyTorch default.

## A2 Anomaly score based on SCE

To assign an anomaly score to a candidate image  $\mathbf{x}_c$  based on its preceding images, we optimized a naive Markov-CPC model, with a single optimization step, on the five preceding images. We then used the prediction error (Eq. 1) of the candidate image  $\epsilon_{K,c}$  and the prediction errors of consecutive image pairs taken from the five preceding images  $\epsilon_p$ , to define the candidate’s anomaly score  $s_c$ :

$$s_c = \frac{\epsilon_{K,c} - \langle \epsilon_p \rangle}{\text{std}(\epsilon_p)} \quad (3)$$

where

$$\langle \epsilon_p \rangle = \frac{1}{K-1} \sum_{i=1}^{K-1} \epsilon_{i,i+1}$$

and  $\text{std}(\epsilon_p)$  is the corresponding standard deviation.

## A3 Model variations

Markov-CPC was implemented with a residual  $T$ , such that  $T(Z(\mathbf{x})) = Z(\mathbf{x}) + \Delta T(Z(\mathbf{x}))$  where  $\Delta T$  is a neural network (see appendix A1). we also tested a variant of Markov-CPC in which  $T$  is non-residual. We found that the performance of a Markov-CPC with a non-residual  $T$  is substantially worse than that with a residual  $T$  (Table t1). This indicates that a residual  $T$  is a good inductive bias for finding these rules.

Model variant	Total accuracy
Residual $T$	$0.52 \pm 0.02$
Non-residual $T$	$0.29 \pm 0.02$

Table t1: Residual versus non-residual  $T$ .

CPC models are usually non-Markovian (Oord et al., 2018; Henaff, 2020). To test the effect of memory on the performance of the CPC model, we used latent variables  $Z$  whose values were also dependent on previous images in the sequence, either via a regular recurrent neural network (RNN) or by an LSTM (Hochreiter & Schmidhuber, 1997). Both the recurrent connections and the LSTM impaired performance, while taking twice the time to compute (Table t2). This indicates that adding recurrent weights to the latent variables, when the data can be explained by Markov latent variables, can impair the ability of the network to extract the rule.

Model variant	Total accuracy	Tests per second
<b>Markov-CPC</b>	<b><math>0.52 \pm 0.02</math></b>	<b><math>13 \pm 2</math> [Hz]</b>
LSTM-CPC	$0.48 \pm 0.02$	$6.6 \pm 0.4$ [Hz]
RNN-CPC	$0.47 \pm 0.02$	$6.6 \pm 0.4$ [Hz]

Table t2: Markov versus recurrent networks. The running times were measured on a basic laptop with Nvidia RTX 2070 GPU.

Throughout the paper, we used Markov-CPC with a 1-dimensional latent space. We tried changing the latent space dimension of Markov-CPC. We found that even a 1-dimensional latent space is enough and that the performance does not strongly depend on this value (Table t3).

Model variant	Total accuracy
Markov-CPC-1D	$0.52 \pm 0.02$
Markov-CPC-10D	$0.53 \pm 0.02$
Markov-CPC-100D	$0.51 \pm 0.02$
Markov-CPC-1000D	$0.50 \pm 0.02$

Table t3: Different  $Z$  latent dimensions.

We also measured the performance of the model without a contrastive loss, minimizing the prediction errors (Eq. 1) of consecutive inputs only (Table t4).

Model variant	Total accuracy
<b>Contrastive loss</b>	<b><math>0.52 \pm 0.02</math></b>
No contrast	$0.45 \pm 0.02$

Table t4: No contrast.

We trained Markov-CPC throughout the paper with an RMSprop optimizer. We also measured the performance with a standard SGD optimizer (Table t5). The optimal learning rate was found to be  $\eta = 40$ .

Model variant	Total accuracy
RMSprop, $\text{lr} = 4 \cdot 10^{-4}$	$0.52 \pm 0.02$
SGD, $\text{lr} = 40$	$0.5 \pm 0.02$

Table t5: SGD.

We also compared the performance of the original RN networks (Sung et al., 2018) to the more shallow networks that we used for Markov-CPC (Fig. f1). The shallower networks were better (Table t6), indicating that in the RN models, simpler networks are better in this task than deeper networks.

Model variant	Total accuracy
<b>Shallow RN (Fig. f1)</b>	<b><math>0.42 \pm 0.02</math></b>
Deep RN (Sung et al., 2018)	$0.27 \pm 0.02$

Table t6: Deep versus shallow RN networks.

Both in the Markov-CPC and RN models, we used a relatively shallow network for the encoder  $Z$  (Fig. f1). We tested other, more complex and deep, networks from the literature as candidate encoder backbones of the Markov-CPC model. The shallow encoder was better than various complicated and deep networks from the literature (Table t7).

Model variant	Total accuracy
<b>Paper's network (Fig. f1)</b>	<b><math>0.52 \pm 0.02</math></b>
VGG11 (Simonyan & Zisserman, 2014)	$0.45 \pm 0.02^*$
DenseNet121 (Huang et al., 2017)	$0.33 \pm 0.02$
AlexNet (Krizhevsky et al., 2012)	$0.31 \pm 0.02$
ResNet18 (He et al., 2016)	$0.29 \pm 0.02^*$
MobileNet v3 small (Howard et al., 2017)	$0.29 \pm 0.02$

Table t7: Encoder Z networks comparison. \*ResNet18 and VGG11 achieved relatively high accuracy on the color rule ( $0.47 \pm 0.03$  and  $0.78 \pm 0.03$  respectively).